The 2010 IEEE/RSJ International Conference on
Intelligent Robots and Systems
October 18-22, 2010, Taipei, Taiwan

Stability Analysis of Robot Motions driven by McKibben Pneumatic Actuator

Yasuhiro Sugimoto, Keisuke Naniwa and Koichi Osuka

Abstract— **It is well known that a robot driven by a McKibben pneumatic actuator generates stable motion in spite of its simple control and simple actuator model. However, how the characteristics of the McKibben pneumatic actuator act on the stability of a robots motion has not been sufficiently discussed. In this paper, a physical model of the McKibben pneumatic actuator is derived and the stability of a robot which is driven by the McKibben pneumatic actuator is analyzed.**

I. INTRODUCTION

Recently, soft actuators have attracted attention for application to robots, and many studies of soft actuators have been conducted. In this research, the McKibben pneumatic actuator in partilular has been focused on.

Introduced in 1957 J. L. McKibben to actuate an orthotic device for handicapped people [1][2], this actuator is a compliant mechanical actuator and is often used as part of an artificial muscle. It consists of a rubber bladder surrounded by a helically braided sleeve and is driven by air pressure. It has a very good characteristics as a soft actuator. (1) It is very lightweight and has a high force-to-weight ratio compared with other actuators. (2) It is comparatively safe even if it breaks down because it uses air pressure as an energy source. (3) It is possible to flexibly correspond it to outside force. Based on the above features, the McKibben pneumatic actuator has often been used for rehabilitations, and power-assistance-suits. Moreover, it has come to be used for actuators of various robots [3][4][5][6][7]. This is because robots actuated by McKibben pneumatic actuators can achieve comparatively stable motions without complicated controls.

As mentioned, it is empirically well known that McKibben pneumatic actuators have various good characteristics and the research of modeling of the McKibben pneumatic actuators has been conducted[8][9][10][11][12]. Although the modeling of the McKibben pneumatic actuator itself was achieved relatively well, what features of the actuator are important and how the features influence stable robot motion have not yet been fully discussed. Thus, in many cases, robots in which McKibben pneumatic actuators were designed and controlled based on a rule of thumb.

Then, the purpose of our research is to analyze how various characteristics of the actuator influence the stability of the movement generated by the McKibben pneumatic actuator and to reveal the features of the McKibben pneumatic actuator that can be used for more sophisticated implementation. As the first step, in this paper, a model of the McKibben pneumatic actuator is derived, in which the characteristics of the actuator are considered Although this model is based on the model in previous research, the formulation is appropriate for a stability analysis. Next, the actuator model is applied to a simple robot model and the stability of motions generated by the actuators is analyzed.

Y. Sugimoto and K. Osuka are with Dept. of Mechanical Engineering, Osaka Univ. {yas, osuka}@mech.eng.osaka-u.ac.jp
K. Naniwa is with Dept. of Mechanical Engineering, Kobe Univ. naniwa@stu.kobe-u.ac.jp

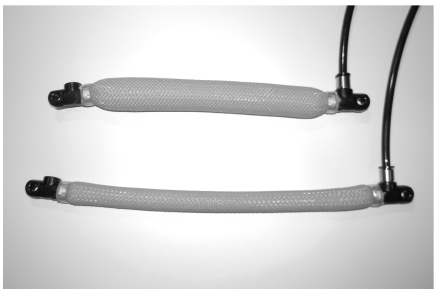

Fig. 1. McKibben actuator with exterior braid and inner elastic bladder

II. MCKIBBEN PNEUMATIC ACTUATOR

An example of the McKibben pneumatic actuator is shown in Fig. 1. The actuator consists chiefly of two components. There is a silicon rubber tube inside and it is surrounded with a mesh of nylon fibers. Actuation is achieved by supplying compressed air into a bladder in the rubber tube. The compressed air expands the bladder and then the volume of the bladder expands. As the volume of the inner bladder increases, the mesh of nylon fibers changes length because the mesh of nylon fibers is not extendable laterally. From this mechanism, the McKibben pneumatic actuator can produce tension and become "an actuator." The fiber used in the actuator has not only softness but also a strong stiffness in the direction of the fiber. By building a mesh structure with the fiber, changeable stiffness, lightness, nonlinear elasticity and physical flexibility can be achieved.

As a defect, an accurate physical modeling or an accurate point-to-point control with the actuator is quite difficult because there are many nonlinear factors in the component of the actuator. However, even with not so complicated control or control depending on insufficient modeling, advanced robot operations could be achieved realized [3][4][5][6]. Although the sophisticated design and mechanism of their robots are one big factors, the proprieties of the actuator, in particular elasticity and viscosity, also seem to affect the

achievement of stable robot motions. Thus, these properities have to be revealed for more sophisticated applications of the McKibben pneumatic actuator.

III. Static Modeling of the McKibben Pneumatic Actuator

As described in the previous section, an accurate modeling of the McKibben pneumatic actuator is very difficult. Although it is possible to develop a model in which the detailed characteristics of the actuator known by the previous work[8] are considered, the derived model become too complex and then it is difficult to understand what character of the McKibben pneumatic actuator contributes to the stability of the movement. Thus, first of all, a simple physical model of the force of actuator is derived according to the air pressure, which is thought to be the most important element for output to the actuator. Next, a slightly complicated physical model was derived. In this model, a force based on the elasticity of the McKibben pneumatic actuator is added. Both the force based on the air pressure and the force based on the elasticity of silicon rubber is assumed to be dependent on the air pressure and the actuator length. However, it is also assumed that these forces are independent on a contractile velocity of the actuator. As a result, the semi-static force generation mechanism can be modeled. In these modelings, a similar technique in some previous work[9] was used. However, to analyze the stability of robots in which the actuator is applied, we derive a different formulation. In the formulation, the relationship between the actuator length, the air pressure and the force is derived explicitly and then the stability analysis of robots can be achieved more easily.

A. Static physical model of McKibben pneumatic actuator

This section describes a static physical model powered by the air pressure of the McKibben pneumatic actuator. However, a detailed geometrical framework is disregarded for simplification. The McKibben Pneumatic actuator consists of a rubber bladder enclosed by helically braided shell. When the bladder is pressured, the volume of bladder with the braided shell expands. As the volume of inner bladder increases, the braided shell changes its length and radius by increasing the pitch angle since the braided fibers are not extendable. In order to formulate a force as a function of air pressure and actuator length without considering a detailed geometric structure, a theoretical approach based on energy conservation is used, as done by Chou and Hannaford[9].

Let a work in which the air pushes the inside of the bladder be W_{in}. W_{in} can be derived as follows:

$$dW_{in} = \int_{S_i} (P - P_0) d\mathbf{l_i} \cdot d\mathbf{s_i} = P' dV_b, \tag{1}$$

where P is the absolute internal air pressure, P_0 is the environment pressure, $P' = P - P_0$ is the relative pressure, S_i is the total inside surface area of the bladder, $d\mathbf{s_i}$ is the amount of the change of the inside surface area, $d\mathbf{l_i}$ is the inner surface displacement and dV_b is the change of the bladder volume.

The output work W_{out} is done when the actuator shortens associated with the volume change, which is:

$$dW_{out} = -f_m dL \tag{2}$$

where f_m is the axial actuator tension (direction of the inside is positive) and dL is axial displacement (direction of the outside is positive). If there is no energy loss by the transformation:

$$dW_{in} = dW_{out} \tag{3}$$

can be derived from the energy conservation law.

Then Eq. (1) and (2) lead:

$$f_m = -P' \frac{dV_b}{dL}. \tag{4}$$

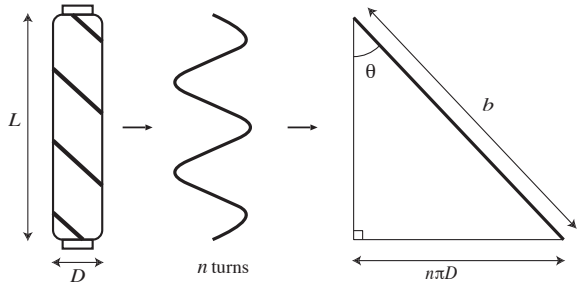

Fig. 2. The geometry of the actuator. The middle segment of the actuator is modeled as a perfect cylinder where length of the actuator is L, diameter is D. n is a number of turns of a thread and b is a thread length. The relationship between the above parameters is illustrated by the triangle.

To formulate dV_b/dL, a central part of the actuator is modeled as a complete cylinder (Fig. 2), where L is the actuator's length, D is the diameter of bladder, n is number of turns of a thread and b is the thread length. The relation between L and D can be expressed by using n and b as:

$$D^2 = \frac{b^2 - L^2}{n^2 \pi^2}. \tag{5}$$

The volume of the bladder is:

$$V_b = \frac{1}{4}\pi D^2 L = \frac{1}{4\pi n^2}(b^2 L - L^3). \tag{6}$$

From Eq. (5) and Eq. (4), the tension f_m can be expressed as the function of P' and L as follows:

$$f_m = -P' \frac{dV_b}{dL} = \frac{P'}{4\pi n^2}(3L^2 - b^2). \tag{7}$$

In this model Eq. (7), the tension f_m is proportional to the air pressure P' and a monotonous function with the length L. Only P' and L are variable and other parameters are fixed. Then, the tension f_m of the actuator can be determined only with the actuator length L and the actuator pressure P'.

B. Adding Series Elasticity

In this section, the model of the actuator(Eq. (3)) is extended by introducing an elastic energy depending on the transformation as follows:

$$dW_{in} = dW_{out} + V_r dW, \tag{8}$$

where V_r is the volume occupied by the bladder and W is the strain energy density function.

From Eq. (8), the actuator tension f_m becomes:

$$f_m = -P' \frac{dV_b}{dL} + V_r \frac{dW}{dL}. \tag{9}$$

The silicon rubber, which is one of the elements of McKibben pneumatic actuators, is a nonlinearly elastic material with large deformation. Such nonlinearly elastic material with large deformation is often said to be "a hyperelastic body." Thus, it is better to formulate a strain energy density function W in the elasticity body model with an appropriate hyperelastic body model. In previous work, the rubber part was modeled by using the Moony-Rivlin model[10] [11]. We also refer to the method in the present study. However, for the following discussion, we derive the improved model so that the relationship between the actuator length and the actuator tension is explicit.

Using the assumptions of initial isotropy and incompressibility, the strain energy density function W can be described with main strain variables $\lambda_i (i = 1,2,3)$ as:

$$W = C_1(\lambda_1^2 + \lambda_2^2 + \lambda_3^2 - 3) + C_2(\frac{1}{\lambda_1^2} + \frac{1}{\lambda_2^2} + \frac{1}{\lambda_3^2} - 3). \tag{10}$$

C_1 and C_2 in Eq. (10) are Mooney-Rivlin constants decided only depending on physical properties of the elastic body. λ_1, λ_2 and λ_3 are described based on the incompressibility of the elastic deformation and λ_2 can be described with L as follows by Eq. (5):

$$\lambda_1 = \frac{L}{L_0},\ \lambda_2 = \frac{D}{D_0} = \frac{1}{D_0 n\pi}\sqrt{b^2 - L^2},\ \lambda_3 = \frac{1}{\lambda_1 \lambda_2}, \tag{11}$$

where L_0 is an initial actuator length and D_0 is an initial actuator outside diameter.

Eq. (10) W can be rewriten by using Eq. (11) :

$$\begin{aligned} W = {} & C_1(\frac{L^2}{L_0^2} + \frac{b^2 - L^2}{D_0^2 n^2 \pi^2} + \frac{L_0^2 D_0^2 n^2 \pi^2}{L^2(b^2 - L^2)} - 3) \\ & + C_2(\frac{L_0^2}{L^2} + \frac{D_0^2 n^2 \pi^2}{b^2 - L^2} + \frac{L^2(b^2 - L^2)}{L_0^2 D_0^2 n^2 \pi^2} - 3). \end{aligned} \tag{12}$$

By substituting Eq. (12) into Eq. (9):

$$\begin{aligned} f_m = {} & -P' \frac{dV_b}{dL} \\ & + V_r \left(C_1 \left(\frac{2L}{L_0^2} - \frac{2L}{D_0^2 n^2 \pi^2} - \frac{2L_0^2 D_0^2 n^2 \pi^2 (b^2 - 2L^2)}{L^3 (b^2 - L^2)^2} \right) \right. \\ & \left. + C_2 \left(-\frac{2L_0^2}{L^3} + \frac{2D_0^2 n^2 \pi^2 L}{(b^2 - L^2)^2} + \frac{2Lb^2 - 4L^3}{L_0^2 D_0^2 n^2 \pi^2} \right) \right), \end{aligned} \tag{13}$$

can be derived.

Similar to the previous actuator model (7), the actuator model (13) depends on only two variables (actuator length L and actuator pressure P').

TABLE I

THE PROPERTIES OF MCKIBBEN PNEUMATIC ARTIFICIAL MUSCLE

Properties	Values	Unit	
b	0.241	m	Braid length
n	3		Number of turns
L_0	0.208	m	Actuator's resting state length
D_0	0.013	m	Actuator's resting state diameter
C_1	192	kPa	Mooney-Rivlin constant
C_2	1.3	kPa	Mooney-Rivlin constant
t_0	0.0015	m	Bladder thickness

IV. VALIDATION OF ACTUATOR MODELS

To confirm how the constructed actuator models in the previous section show the characteristics of the actual McKibben pneumatic actuator, model validation experiments were carried out with real McKibben pneumatic actuators. The experimental setup is shown in Fig. 3 and 4.

Fig. 5(a) and 5(b) show the relation between the actuator shrinkage and the air pressure under constant loads. In this figure, the calculation result only with the air pressure (model 1, Eq. (7)), the calculation result with the air pressure and elasticity (model 2, Eq. (13)) and the experimental data are shown. The parameters of the actuator used for the calculation are shown in Table I.

From Fig. 5(a) and 5(b), it is difficult to say that model 1, which considered only the air pressure of the actuator, shows a similar property to the experimental data. On the other hand, model 2, in which not only the air pressure but also elasticity were considered, shows very similar characteristics to the real McKibben pneumatic actuator. Thus, it can be said that model 2 (Eq. (13)) is able to express the property of the McKibben pneumatic actuator relatively well even though the model is not so complicated.

However, the actuator models (both model 1 & model 2) did not draw a hysteresis loop although a hysteresis loop was shown in the experimental result according to the difference between the pressurizing process and the decompressing process. This is because they did not consider the difference between the pressurizing and the decompressing process in their models. The hysteresis loop can be expressed by adding the frictional element to the actuator model, which depends on the friction between the fibers and the actuator surroundings. With such a model, we will be able to derive a more precise actuator model. However, such a model will be more complicated and then it will be quite difficult to analyze the robot's motions as applied to the McKibben

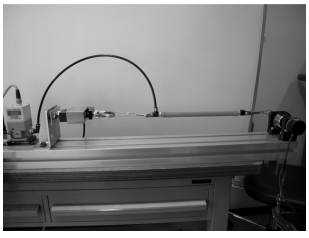

Fig. 3. Experimental setup

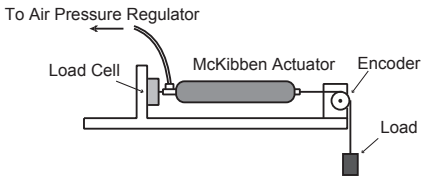

Fig. 4. Experimental setup components

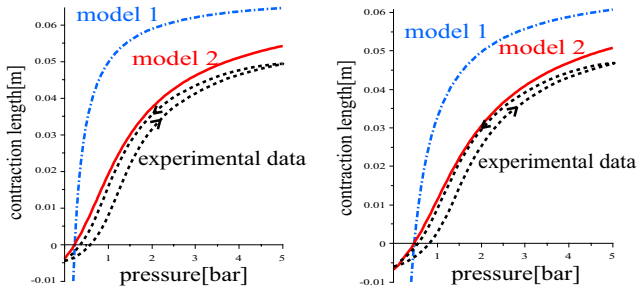

(a) 15N (b) 30N

Fig. 5. Relation between contraction and pressure

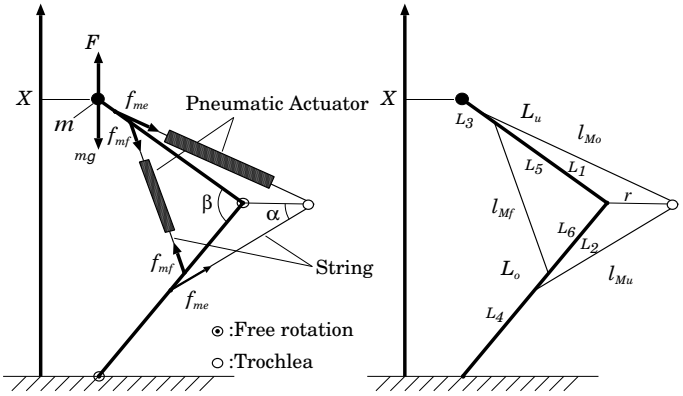

Fig. 6. Model of the knee pneumatic actuator group

pneumatic actuators. Therefore, we assume that model (13), which considered the elastomeric force of rubber and the air pressure can show a static characteristic of the actuator sufficiency and we adopt the model in the following section.

V. Two dimensional model of robot leg

In this section, the robot model in which the McKibben pneumatic actuator is applied is derived. Using the robot model and the McKibben pneumatic actuator model (13), we analyze the stability of the motions in the next section. To clarify the mechanical characteristics of the McKibben pneumatic actuator, it is necessary to choose an adequately simple and easily comprehensible model. Thus, we adopt a two dimensional model of the leg robot that contains a minimum element (See Fig. 6). This model is the same as the one used in the research that considers the mechanical characteristics of an actual muscle-skeletal system to muscular stability [13][14]. In this model, an antagonistic pair of McKibben pneumatic actuators is arranged around the knee. Bending and stretching movement in a perpendicular direction can be achieved by bending the knee. Each symbol and link length in the figure is shown in the appendix.

To simplify the following discussion, the motion of the representative mass of the leg and hip (m in Fig. 6) is assumed to be constrained in a vertical one-dimensional movement, that is the hip does not move horizontally.

The geometric transformation between the ground reaction force F and the actuator forces f_{me} and f_{mf} for vertical movements can be described as:

$$F(X,P'_e,P'_f) = G_e(X)f_{me}(L_e,P'_e) - G_f(X)f_{mf}(L_f,P'_f). \quad (14)$$

The geometric functions $G_e(X)$ and $G_f(X)$ in Eq. (14) can be derived from the equilibration of the moment of the robot as:

$$G_e(X) = \frac{r\sin\alpha}{L_oL_u\sin\beta}X, \quad (15)$$

$$G_f(X) = \frac{L_5L_6}{L_oL_ul_{mf}}X. \quad (16)$$

The dynamical equation of the system can be described as:

$$\begin{pmatrix}\dot{X}\\ \dot{V}\end{pmatrix} = \begin{pmatrix}V\\ (1/m)F(X,P'_e,P'_f) - g\end{pmatrix}. \quad (17)$$

where V is vertical velocity of the hip, L_e, P'_e are length and pressure of actuator that virtually act as extensor muscle, L_f, P'_f are length and pressure of the actuator that virtually acts as flexor muscle and g is the gravitational acceleration.

VI. Stability analysis

A. Stability criteria

In this section, the stability for the constant posture of the robot is analyzed. That is, it is analyzed as to whether the robot can return to its former posture after a small disturbance.

Linearizing the system of Eq. (17), the following system can be derived:

$$\frac{1}{dt}\begin{pmatrix}X\\ V\end{pmatrix} = \begin{pmatrix}0 & 1\\ a_2 & a_1\end{pmatrix}\begin{pmatrix}X\\ V\end{pmatrix}. \quad (18)$$

where

$$a_2 = \frac{1}{m}\frac{\partial}{\partial X}\left(G_e(X)f_{me}(L_e,P'_e) - G_f(X)f_{mf}(L_f,P'_f)\right),$$

$$a_1 = \frac{1}{m}\frac{\partial}{\partial V}\left(G_e(X)f_{me}(L_e,P'_e) - G_f(X)f_{mf}(L_f,P'_f)\right).$$

By using the Jacobian of Eq. (18), the conditions of local stability can be derived based on the well-known Routh-Hurwiz criterion. Such a stability criterion can be derived as follows:

$$a_1 < 0, \quad (19)$$

$$a_2 < 0. \quad (20)$$

With these conditions (19), (20), the local stability analysis of the system can be achieved.

B. Stability of robot leg posture

In this section, we investigate whether the robot with the constructed actuator (13) can satisfy the condition given by Eq. (19) and (20).

First, we investigate the second condition of stability (20). The differentiation F with X is very difficult. Thus, by using the following geometrical relationship, X, L_e and L_f were

translated to the functions as α. With the translated functions, Eq. (20) can be rewritten as:

$$\begin{aligned} &\frac{1}{m}\frac{\partial}{\partial X}\left(G_e(X)f_{me}(L_e,P'_e)-G_f(X)f_{mf}(L_f,P'_f)\right)<0 \\ \Longleftrightarrow\ &\frac{\partial\alpha}{\partial X}\frac{\partial}{\partial\alpha}\left(G_e(\alpha)f_{me}(\alpha,P'_e)-G_f(\alpha)f_{mf}(\alpha,P'_f)\right)<0. \end{aligned} \tag{21}$$

X is a monotone increasing for the range of α. Then, the inequality:

$$h(\alpha,P'_e,P'_f)<0 \tag{22}$$

becomes the necessary and sufficient condition for Eq. (20) where:

$$\begin{aligned} h(\alpha,P'_e,P'_f) &= \frac{\partial}{\partial\alpha}\left(G_e(\alpha)f_{me}(\alpha,P'_e)-G_f(\alpha)f_{mf}(\alpha,P'_f)\right) \\ &= \frac{\partial G_e(\alpha)}{\partial\alpha}f_{me}(\alpha,P'_e)+G_e(\alpha)\left(-P'_e\frac{\partial}{\partial\alpha}\frac{dV_b}{dL_e}+V_r\frac{\partial}{\partial\alpha}\frac{dW}{dL_e}\right) \\ &-\left(\frac{\partial G_f(\alpha)}{\partial\alpha}f_{mf}(\alpha,P'_f)+G_f(\alpha)\left(-P'_f\frac{\partial}{\partial\alpha}\frac{dV_b}{dL_f}+V_r\frac{\partial}{\partial\alpha}\frac{dW}{dL_f}\right)\right). \end{aligned} \tag{23}$$

Then, the set which satisfies $h(\alpha,P'_e,P'_f)=0$ can be calculated and $h(\alpha,P'_e,P'_f)$ is monotonically decreased along the α axis. The result was shown in Fig. 7. The area above the surface $h(\alpha,P'_e,P'_f)=0$ is satisfied by $h(\alpha,P'_e,P'_f)<0$. In the same Figure, the set which satisfies $V=0$, that is, the set of an equilibrium point of the system (18) is also shown. In the range of $0<\alpha<\pi/2$, the plane of $h(\alpha,P'_e,P'_f)=0$ was obtained only one set[1]. From this result, it can be said that the set of equilibrium point at the upper region of plane $h(\alpha,P'_e,P'_f)=0$ satisfies the condition (22). On the other hand, equilibrium points at the lower region of plane $h(\alpha,P'_e,P'_f)=0$ do not satisfy the condition (22). However, in such a situation, the knee joint angle α becomes small. This means that the knee is greatly bent. Though an animal's muscle is capable of such extension, the McKibben actuator is not. Thus, this posture, in which the knee is greatly bent and the extensor is greatly extended, can not be achieved. Therefore, equilibrium points at the lower region of plane $h(\alpha,P'_e,P'_f)=0$ can not be realized because of the limited range of knee motion. From these facts, it can be said that the stability condition (20) can be satisfied for the actuator model (13).

In order to satisfy Eq. (22), the sum of the second and third expression in Eq. (23) should be negative. The value for terms in expression (23) can be calculated and the important terms in the result are Eq. (24) and (25). Due to Eq. (24) and (25), the sum of the second and third term becomes negative.

$$-P'_e\frac{\partial}{\partial\alpha}\frac{dV_b}{dL_e}<0,\quad V_r\frac{\partial}{\partial\alpha}\frac{dW}{dL_e}<0, \tag{24}$$

$$-P'_f\frac{\partial}{\partial\alpha}\frac{dV_b}{dL_f}>0,\quad V_r\frac{\partial}{\partial\alpha}\frac{dW}{dL_f}>0. \tag{25}$$

[1]For $0<\alpha<\pi/2$, two planes ware obtained. But one of these plane is physically impossible because of the range of knee motion.

TABLE II

THE PROPERTIES OF THE MODEL OF KNEE

Properties	Values	Unit
m	10	kg
L_1	0.55	m
L_2	0.08	m
L_5	0.21	m
L_6	0.05	m
L_o	0.44	m
L_u	0.43	m
L_{ec}	0.52	m
L_{fc}	0.05	m
r	0.059	m

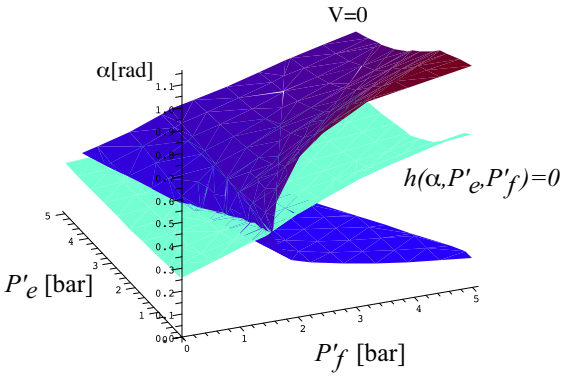

Fig. 7. The plane of $h(\alpha,P'_e,P'_f)=0$ and $V=0$

These facts are due to the properties of elastic and pneumatic materials. Therefore, it can be determined that these properties have an overall positive effect on stability. Indeed, by ignoring other factors in the static model of the actuator, Eq. (24) and (25) may be not satisfied. However, from the static experiments, it is known that the dominant forces in the actuator come from the elastic and the pressure elements, so this approximation seems to be reasonable. This is an intuitive result when taking into consideration the natural characteristics of springs and pneumatic cylinders. However, the stability is also greatly influenced by the choice of robot model. On the other hand, Eq. (19) can be written as:

$$\frac{1}{m}\frac{\partial}{\partial V}\left(G_e(X)f_{me}(L_e,P'_e)-G_f(X)f_{mf}(L_f,P'_f)\right)<0. \tag{26}$$

The actuator model (13), which is derived in the previous section, does not include the velocity-tension dependency and depends only on the actuator length and inner pressure. Therefore, the differentiation F with V becomes 0 and it cannot be said that the condition (19) is satisfied. However, in experimental results for McKibben pneumatic actuators in previous research[11], the velocity-tension relationship of the McKibben pneumatic actuator monotonically decreased although its gradient is quite small. This result indicates that the condition (19) may be satisfied by the properties not included in the derived model (13). Indeed, results from the experiment shown in Fig. 5(a) and 5(b) indicate a hysteresis loop. If it has a hysteresis loop, there must also be a dissipation term such as viscous dampening or friction.

Therefore, the differentiation F with V becomes negative and it can be qualitatively said that the condition (19) will be satisfied. In order to quantify this, the velocity-tension relationship needs to be investigated as future work.

VII. Conclusion

In this paper, a model of a McKibben pneumatic actuator, in which the air pressure and the elasticity of the actuator were taken into account was first derived. It was then compared with the experimental data, and confirmed to be sufficiently accurate. Thus, the air pressure and the elasticity are dominant in actuator's static characeristics. Next, the stability of motions for a simple knee bending robot driven by the McKibben pneumatic actuator was analyzed. As a result, it was shown that the motion generated by the derived model, in which both the air pressure and the elasticity were considered, could satisfy the conditions of the length-tension relationship.

However, the stability condition concerning the velocity was not satisfied because the velocity-tension relationship of the actuator was not included in the derived actuator model. As mentioned, it seems that there is a relationship between the tension in the McKibben pneumatic actuator, viscous forces, and contractile velocity. Therefore, it is necessary to construct an extended actuator model in which the velocity dependence characteristics are included.

Additionally, the dynamics of the actuator air was not considered as we approximated P' to be constant, and actuation to be instantaneous. In reality, the McKibben actuator's internal air pressure varies and there is a time delay when the robot is operated. Therefore, it is also necessary to discuss the impact these things could have on the model.

ACKNOWLEDGMENTS

This work has been partially supported by a Grant-in-Aid for Scientific Research on Priority Areas "Emergence of Adaptive Motor Function through Interaction betweenBody, Brain and Environment" from the Japanese Ministry of Education, Culture, Sports, Science and Technology.

References

[1] H. Schulte, "The characteristics of the McKibben artificial muscle," *The application of external power in prosthetics and orthotics*, pp. 94–115, 1961.

[2] V. Nickel, J. Perry, and A. Garrett, "Development of useful function in the severely paralyzed hand," *Journal of Bone and Joint Surgery*, vol. 45, no. 5, pp. 933–952, 1963.

[3] S. Collins, A. Ruina, R. Tedrake, and M. Wisse, "Efficient bipedal robots based on passive-dynamic walkers," *Science*, vol. 307, no. 5712, p. 1082, 2005.

[4] M. Wisse and R. van der Linde, *Delft Pneumatic Bipeds*. Springer Tracts In Advanced Robotics, 2007.

[5] T. Takuma and K. Hosoda, "Controlling the walking period of a pneumatic muscle walker," *The International Journal of Robotics Research*, vol. 25, no. 9, p. 861, 2006.

[6] R. Niiyama, A. Nagakubo, and Y. Kuniyoshi, "Mowgli: A bipedal jumping and landing robot with an artificial musculoskeletal system," in *2007 IEEE International Conference on Robotics and Automation*. Citeseer, 2007, pp. 2546–2551.

[7] K. Hosoda, T. Takuma, A. Nakamoto, and S. Hayashi, "Biped robot design powered by antagonistic pneumatic actuators for multi-modal locomotion," *Robotics and Autonomous Systems*, vol. 56, no. 1, pp. 46–53, 2008.

[8] B. Tondu and P. Lopez, "Modeling and control of McKibben artificial muscle robot actuators," *IEEE Control Systems Magazine*, vol. 20, no. 2, pp. 15–38, 2000.

[9] C. Chou and B. Hannaford, "Measurement and modeling of McKibben pneumatic artificial muscles," *IEEE Transactions on robotics and automation*, vol. 12, no. 1, pp. 90–102, 1996.

[10] G. Klute and B. Hannaford, "Accounting for elastic energy storage in McKibben artificial muscle actuators," *Journal of Dynamic Systems, Measurement, and Control*, vol. 122, p. 386, 2000.

[11] G. Klute, J. Czerniecki, and B. Hannaford, "Artificial muscles: Actuators for biorobotic systems," *The International Journal of Robotics Research*, vol. 21, no. 4, p. 295, 2002.

[12] M. Doumit, A. Fahim, and M. Munro, "Analytical Modeling and Experimental Validation of the Braided Pneumatic Muscle," *IEEE transactions on robotics*, vol. 25, no. 6, pp. 1282–1291, 2009.

[13] H.Wagner and R.Blickhan, "stabilizing function of antagonistic neuromusculoskeletal systems: an analytical investigation," *Biological Cybernetics*, vol. 89, pp. 71–79, 2003.

[14] Y. Sugimoto, S. Aoi, N. Ogihara, and K. Tsuchiya, "Stabilizing Function of the Musculoskeletal System for Periodic Motion," *Advanced Robotics*, vol. 23, no. 5, pp. 521–534, 2009.

APPENDIX

A. List of Symbols

L_o: Length from knee to waist
L_u: Lower link length
L_1: Length the link to the outside actuator installation positions from the knee
L_2: Length the link to the outside actuator installation positions from the knee
L_3: Length the link from the outside actuator installation position to the waist
L_4: Length the link from the outside actuator installation position to the ankle
L_5: Length the link from the inside actuator installation position to the knee
L_6: Length the link from the inside actuator installation position to the knee
l_{Mo}: Outside actuator length from thigh to kneecap
l_{Mu}: Outside actuator length from leg to kneecap
l_{Mf}: Inside actuator length
r: Length of link from knee to kneecaps
α: Turning angle of kneecap
β: Turning angle of knee
m: Body mass
X: Vertical displacement of the location of the waist
f_{me}: Extensor(outside) actuator tension
f_{mf}: Flexor(inside) actuator tension